

# Orbital Specific Charge Transfer Distances, Solvent Reorganization Energies, and Electronic Coupling Energies: Electronic Stark Effect Studies of Parallel and Orthogonal Intervalence Transfer in $(\text{NC})_5\text{Os}^{\text{II}}-\text{CN}-\text{Ru}^{\text{III}}(\text{NH}_3)_5^-$

Laba Karki and Joseph T. Hupp\*

Contribution from the Department of Chemistry, Northwestern University, Evanston, Illinois 60208

Received September 18, 1996<sup>⊗</sup>

**Abstract:** For the mixed-valent chromophore,  $(\text{NC})_5\text{Os}^{\text{II}}-\text{CN}-\text{Ru}^{\text{III}}(\text{NH}_3)_5^-$ , spin-orbit coupling and ligand-field asymmetry effects lead to multiple visible region intervalence (metal-to-metal) charge transfer transitions (Forlando et al. *Inorg. Chim. Acta* **1994**, 223, 37). The higher energy transition is associated with transfer from an Os  $5d\pi$  orbital that is nominally orthogonal to the charge transfer axis. The lower energy transition, on the other hand, involves a degenerate pair of Os  $5d\pi$  donor orbitals directed along the charge transfer axis. Low-temperature electronic Stark effect measurements of the partially resolved transitions permit donor-orbital-specific one-electron-transfer distances to be directly evaluated. The distances,  $R$ , are remarkably dependent upon donor orbital orientation ( $R(\text{parallel}) = 2.8 \pm 0.2 \text{ \AA}$ ;  $R(\text{orthogonal}) = 4.0 \pm 0.4 \text{ \AA}$ ) and significantly shorter than simple geometric estimates (5.0  $\text{\AA}$ ). From the distance information, donor-orbital-specific coupling energies and solvent reorganization energies can also be estimated. These also differ substantially from those obtained by equating the charge transfer distance with the geometric donor/acceptor separation distance.

## Introduction

Electronic coupling, solvent reorganization, and the distance of charge transfer are factors of central significance in the kinetics of nearly all molecule based electron transfer reactions.<sup>1</sup> The magnitude and, therefore, absolute quantitative influence of each can depend on an enormously wide variety of donor, acceptor, and bridge structural and chemical compositional considerations. Here we report new experimental studies that elucidate, within a single assembly, the dependence of these crucial parameters on donor orbital orientation and identity. The system examined was a bridged mixed valence assembly,  $(\text{NC})_5\text{Os}^{\text{II}}-\text{CN}-\text{Ru}^{\text{III}}(\text{NH}_3)_5^-$ .<sup>2</sup> In this assembly the available donor orbitals are the nominally degenerate  $5d\pi$  orbitals of the osmium center. Two of these orbitals ( $d_{xz}$  and  $d_{yz}$ ) are directed along the metal-metal charge transfer axis ( $z$  axis). The third ( $d_{xy}$ ) is geometrically orthogonal. Spin-orbit coupling together with bridge-induced ligand-field asymmetry partially lifts the degeneracy (Scheme 1). The spin-orbit perturbation also partially mixes the orbitals and thereby relaxes the charge transfer orthogonality associated with the  $d_{xy}$  orbital.<sup>3</sup>

To interrogate the orbital specificity of the charge transfer process we have taken advantage of the corresponding spin-orbit induced splitting of the visible-region intervalence transition (eq 1). We have then probed the component transitions by resonance Raman and electronic Stark effect spectroscopies.

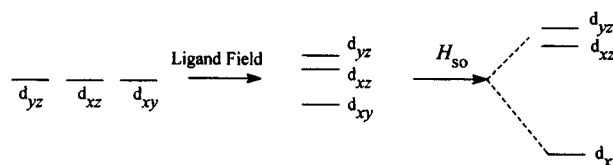
<sup>⊗</sup> Abstract published in *Advance ACS Abstracts*, April 1, 1997.

(1) For reviews see: (a) Creutz, C. *Prog. Inorg. Chem.* **1983**, 30, 1. (b) Newton, M. D.; Sutin, N. *Annu. Rev. Phys. Chem.* **1984**, 35, 437. (c) Newton, M. D. *Chem. Rev.* **1991**, 91, 767. (d) Crutchley, R. J. *Adv. Inorg. Chem.* **1994**, 41, 273.

(2) (a) Forlando, P.; Baraldo, L. M.; Olabe, J. A.; Della Vedova, C. O. *Inorg. Chim. Acta* **1994**, 223, 37–42. (b) Vogler, A.; Klissinger, J. *J. Am. Chem. Soc.* **1982**, 104, 2311. (c) Vogler, A.; Osman, A. H.; Kunkley, H. C. *Coord. Chem. Rev.* **1985**, 64, 159.

(3) (a) Curtis, J. C.; Meyer, T. J. *Inorg. Chem.* **1982**, 21, 1562. (b) Kober, E. M.; Goldsby, K. A.; Narayana, D. N. S.; Meyer, T. J. *J. Am. Chem. Soc.* **1983**, 105, 4303. (c) Karki, L.; Lu, H. P.; Hupp, J. T. *J. Phys. Chem.* **1996**, 100, 15637.

## Scheme 1



As indicated below, the former establishes the identities of the donor orbitals while the latter provides direct measures of the effective charge transfer distances. From the measurements and related analyses we find that orbital-specific electron-transfer distances, coupling energies, and reorganization energies can indeed be evaluated and that these parameters can depend strongly upon orbital identity.

## Experimental Section

$(\text{Na})[(\text{NC})_5\text{Os}^{\text{II}}-\text{CN}-\text{Ru}^{\text{III}}(\text{NH}_3)_5]$  was prepared and purified by a literature method.<sup>2b</sup> Electroabsorption experiments were performed in 100- $\mu\text{m}$  cells in a 50:50 (v/v) ethylene glycol-water matrix at 77 K. Typical root-mean-square electric field strengths (220 Hz) were  $3 \times 10^7 \text{ V/m}$ . Additional details concerning the experimental electroabsorption configuration and the analysis protocol can be found in ref 4.

Local field corrections (vide infra) require an estimate for the static dielectric constant,  $D_s$ , of the spectroscopic matrix. An estimate was obtained from electroabsorption cell capacitances which, in turn, were obtained from a series of impedance measurements (Solaratron 1250/1286 impedance spectrometer) made between 65 kHz and 100 Hz. Because the directly measured capacitance can contain contributions from stray capacitances, the ethylene glycol-water glass dielectric constant was ultimately determined from an experimental capacitance/ $D_s$  calibration curve (Figure 1). From the curve (seven liquids + air),  $D_s$  for the glass is ca. 3.7.

Raman experiments were performed at room temperature in water as solvent by using a Spex triplemate monochromator and a 1 in. CCD camera. Sample excitation was accomplished with either an  $\text{Ar}^+$

(4) Karki, L.; Hupp, J. T. *Inorg. Chem.* In press.

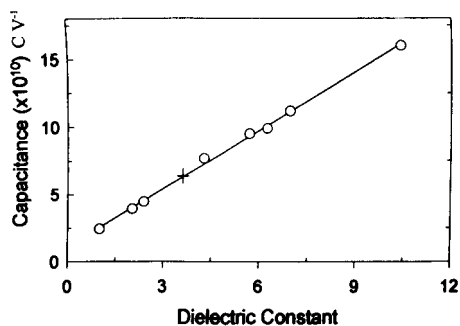


**Figure 1.** Calibration curve of measured cell capacitance versus dielectric constant for air and seven ambient temperature solvents of known dielectric strength (circles). The 77 K dielectric constant of the spectroscopic glass (shown as “+” in the figure) was determined by placing the experimentally determined capacitance on the best-fit line.

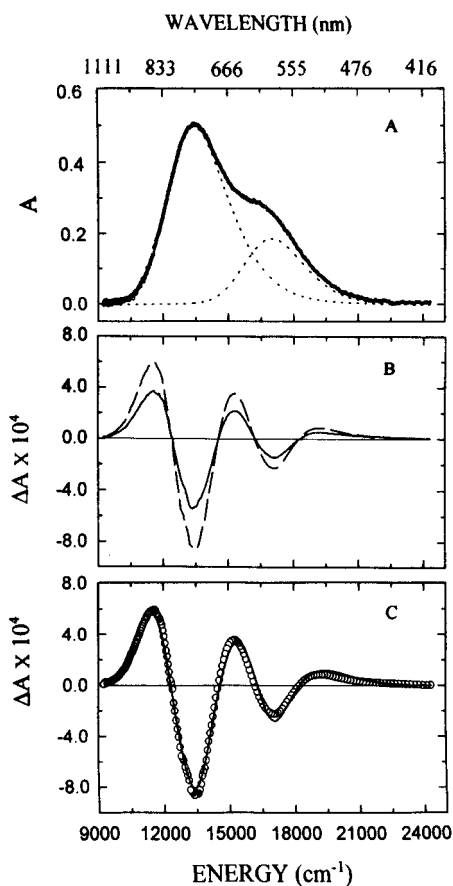


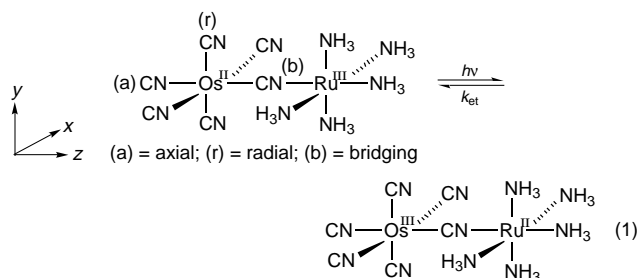
**Figure 2.** Panel A: experimental absorption spectrum at 77 K (circles). Dotted lines show the individual Gaussian transitions and the solid line shows the overall fit (sum of the two fitted transitions). Panel B: Experimental electroabsorption signal at 90° (solid line) and 55° (dashed line) at an external field strength of  $4.03 \times 10^7$  V/m. Panel C: Least-squares fit (solid line) of the 55° electroabsorption spectrum (circles).

pumped titanium-sapphire or dye laser. It should be noted that maxima in the room temperature absorption spectrum (Raman studies) are red shifted by about  $1400 \text{ cm}^{-1}$  from those in the 77 K spectrum (electroabsorption studies).

## Results and Discussion

Figure 2A shows the visible region electronic absorption spectrum for  $(\text{NC})_5\text{Os}^{\text{II}}-\text{CN}-\text{Ru}^{\text{III}}(\text{NH}_3)_5^-$ , where the two features are assigned as overlapping intervalence transitions. Notably, their energy difference ( $\sim 4000 \text{ cm}^{-1}$ ) is close to the expected value of  $3/2$  times the spin-orbit coupling constant for osmium ( $\lambda_{\text{SO}} \approx 3000 \text{ cm}^{-1}$ ).<sup>5,6</sup> Based on ligand field

considerations, the lower energy absorption is assigned to intervalence electron transfer from the degenerate pair of orbitals directed toward the acceptor. The higher energy, lower intensity transition is assigned to charge transfer from the single orthogonal donor orbital. Resonance Raman scattering experiments (830 and 600 nm excitation) confirm the intervalence assignments: Enhanced scattering is observed for vibrations associated with both the donor and acceptor ends of the molecule. Moreover, excitation at 830 nm leads to strong enhancement of scattering from bridging and axial  $\text{C}\equiv\text{N}$  modes (along the charge transfer axis), while excitation at 600 nm preferentially enhances scattering from the equatorial cyanide ligands (normal to the charge transfer axis).



External electric field perturbation of the absorption spectrum provides information about ground state (1)/excited state (2) polarizability changes,  $\Delta\alpha_{12}$ , along the transition moment axis and about absolute changes in dipole moment,  $|\Delta\mu_{12}|$ .<sup>7,8</sup> According to Liptay, the difference spectrum (electroabsorption spectrum) for an orientationally constrained, isotropic sample can be written as a linear combination of zeroth, first, and second derivatives of the unperturbed absorption spectrum:<sup>7,8</sup>

$$\Delta A(\nu) = \left\{ A_x A(\nu) + \frac{B_x}{15hc} \frac{v d[A(\nu)/v]}{d\nu} + \frac{C_x}{30h^2 c^2} \frac{v d^2[A(\nu)/v]}{d\nu^2} \right\} F_{\text{int}}^2 \quad (2)$$

where  $F_{\text{int}}$  is the internal electric field<sup>9</sup> (i.e., the field actually experienced by the chromophore),  $\nu$  is the frequency of the absorbed light,  $h$  is Planck's constant, and  $c$  is the speed of light. The coefficients  $A_x$ ,  $B_x$ , and  $C_x$  have been described in detail elsewhere.<sup>7,8</sup> Briefly, they provide information respectively about the transition moment polarizability and hyperpolarizability,  $\Delta\alpha_{12}$ , and  $\Delta\mu_{12}$ .

Figure 2B shows the experimental Stark spectrum for  $(\text{NC})_5\text{Os}-\text{CN}-\text{Ru}(\text{NH}_3)_5^-$  measured with PMT and Si photodiode detectors at angles of 90° and 55° between the polarized incident light and the applied electric field. Both peaks display the field squared dependence expected from eq 2. Figure 2C shows a six-parameter fit of the 55° spectrum to eq 2 (i.e., zeroth, first, and second derivative spectra for each of two electronic transitions; see Figure 2A for a Gaussian deconvolution of the original absorption spectrum). It should be noted that attempts to fit the Stark spectrum to only three parameters (appropriate

(5) (a) Goodman, B. A.; Raynor, J. B. *Adv. Inorg. Chem. Radiochem.* **1970**, *13*, 192. (b) Hill, N. J. *J. Chem. Soc., Faraday Trans.* **1972**, *68*, 427.

(6) In view of both ligand-field splitting effects and differences in vibrational and solvational reorganization energy (below), exact agreement is not expected.

(7) Liptay, W. In *Excited States*; Lim, E. C., Ed.; Academic Press: New York, 1974; Vol 1, pp 129–229.

(8) (a) Oh, D. H.; Boxer, S. G. *J. Am. Chem. Soc.* **1990**, *112*, 8161. (b) Oh, D. H.; Sano, M.; Boxer, S. G. *J. Am. Chem. Soc.* **1991**, *113*, 6880.

(9) The available dielectric constant data for the spectroscopic matrix used here (Figure 1) yields, in the spherical cavity limit, a local field correction factor of  $3D_s/(2D_s + 1) = 1.31 = F_{\text{int}}/F_{\text{ext}}$ , where  $F_{\text{ext}}$  is the externally applied electric field.

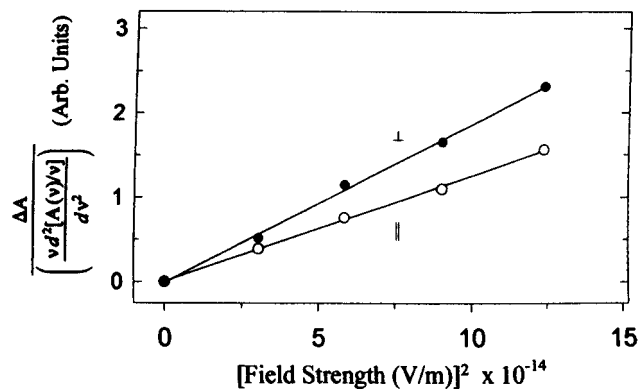


**Figure 3.** Field dependence of Stark signals at 13 500 (squares; parallel transition) and 17 000  $\text{cm}^{-1}$  (circles; perpendicular transition). Note the higher slope for the latter, indicating greater  $|\Delta\mu|$ .

if Figure 2A consisted of a single homogenous electronic transition) were unsuccessful. Qualitatively, the experimental and calculated (fit) Stark spectra are characterized by significant second derivative contributions, indicating that significant changes in dipole moment and, therefore, significant charge transfer accompany the optical excitations. Quantitatively, the parallel and orthogonal charge transfers are characterized by absolute dipole moment changes of  $13.5 \pm 1$  and  $19.5 \pm 2$  D, respectively.<sup>10</sup> The differences are further illustrated in Figure 3, where field strength responses at the two absorbance maxima are shown. Also observed (Figure 2) are significant polarizability changes, where the fitting yields values of the trace of  $\Delta\alpha$  of  $570 \pm 100$  and  $950 \pm 200 \text{ \AA}^3$  for the lower and higher energy transitions, respectively. The positive values indicate that the electronic excited states are more polarizable than the ground state.<sup>11</sup>

Returning to the dipole moment changes, these can be related directly to adiabatic electron transfer distances,  $R_{12}$ , simply by dividing by the unit electronic charge. On this basis the distances are  $2.7 \pm 0.2$  and  $3.9 \pm 0.4 \text{ \AA}$  for charge transfer from the parallel and orthogonal donor orbitals, respectively. Notably, both are less than the estimated geometric donor–acceptor (metal–metal) separation distance of  $5.0 \text{ \AA}$ .<sup>12</sup> One possibility is that the effective distances are short because of significant delocalization of the transferring electron. Application of the so-called “generalized Hush–Mulliken” analysis as prescribed by Newton and Cave<sup>13</sup> leads, however, to nearly identical *nonadiabatic* electron transfer distances,  $R_{ab}$ , i.e.,  $2.8 \pm 0.2$  and  $4.0 \pm 0.4 \text{ \AA}$ . A more probable explanation is that significant polarization and repolarization effects exist for both the transferring electron and other valence electrons.<sup>14</sup> Evidently, the magnitude of such effects depends substantially on whether the photogenerated hole is created in a donor orbital largely orthogonal to the charge transfer axis or one directed toward the bridge and electron acceptor. A third explanation

(10) The angles,  $\xi$ , between the transition dipole moment and the change in dipole moment are  $0^\circ$  for the lower energy transition (expected for a simple charge transfer in a linear donor/bridge/acceptor assembly) and  $15^\circ$  for the higher energy transition. While small, the deviation of the latter angle from  $0^\circ$  is difficult to understand in light of the relatively high symmetry of the electron donor and the likely highly symmetrical spatial distribution of the  $d_{xy}$  donor orbital with respect to the charge transfer axis. Conceivably, the deviation is an artifact attributable to errors in the initial spectral deconvolution.

(11) A previous assignment of a negative sign to the polarizability change for intervalence excitation of a closely related complex was in error, although the reported absolute magnitude of  $\text{Tr}\Delta\alpha$  was correct.<sup>3</sup>

(12) Vance, F. W.; Stern, C. S. Unpublished X-ray crystallographic studies.

(13) (a) Cave, R.; Newton, M. D. *Chem. Phys. Lett.* **1996**, *249*, 15. (b) Creutz, C.; Newton, M. D.; Sutin, N. *J. Photochem. Photobiol. A: Chem.* **1994**, *82*, 47.

for the discrepancy based on  $d_{yz}$  and  $d_{xz}$  orbitals lying closer to the acceptor seems qualitatively incorrect since the orbital center, in every case, is the osmium nucleus. However, Ru(III) almost certainly must differentially polarize and distort the  $d_{yz}$  and  $d_{xz}$  orbitals relative to the  $d_{xy}$  orbital. Relaxation of the  $z$ -directed polarization presumably is more significant in the charge transfer excited state if the photogenerated hole is placed in either the  $d_{xz}$  or  $d_{yz}$  orbital, rather than in the orthogonal  $d_{xy}$  orbital.

The availability of directly measured one-electron transfer distances permits orbital-specific solvent reorganization energies,  $\chi_s$ , to be estimated. To obtain the estimates we treated the donor-bridge-acceptor assembly as an ellipsoid and then employed the dipole-switch/cavity model of Brunschwig et al.,<sup>15</sup> where  $R_{12}$  was equated with the switch length. For ambient temperature water as solvent the results are striking:  $\chi_s$  is  $4700 \text{ cm}^{-1}$  for optical electron transfer from the osmium  $d_{xy}$  orbital, but only  $2550 \text{ cm}^{-1}$  for electron transfer from either the  $d_{xz}$  or  $d_{yz}$  orbital.<sup>16</sup> Notably, both energies are much less than the value calculated by using the full metal–metal separation distance (i.e.,  $\chi_s = 7000 \text{ cm}^{-1}$ ). The smaller measured values have significant implications in terms of both classical and quantum mechanical barriers to back electron transfer.

The combined absorption and electroabsorption measurements also make possible the evaluation of nonadiabatic electronic coupling energies,  $H_{ab}$ . These are given by the energy-weighted ratio of the transition dipole moment,  $\mathbf{P}_{12}$ , to the change in dipole moment:<sup>13</sup>

$$H_{ab} = \frac{\mathbf{P}_{12} \nu_{\max}}{\Delta\mu_{ab}} \quad (3)$$

Noting that  $\mathbf{P}_{12}$  is proportional to the square root of the oscillator strength of the electronic transition and that  $\Delta\mu_{ab}$  is given by the product of the unit electronic charge,  $e$ , and the nonadiabatic charge transfer distance, we can rewrite eq 3 in terms of readily observable parameters:<sup>13</sup>

$$H_{ab} = (2.06 \times 10^{-2}) \left( \frac{\epsilon_{\max} \Delta\nu_{1/2} \nu_{\max}}{e^2 \mathbf{R}_{ab}^2 b} \right)^{1/2} \quad (4)$$

In eq 4,  $\epsilon_{\max}$  is the extinction coefficient,  $\Delta\nu_{1/2}$  is the absorption band width,  $\nu_{\max}$  is the absorption band maximum, and  $b$  is a degeneracy term. Here  $b$  accounts for the possibility of optical ET from multiple degenerate donor orbitals. For the lower energy transition  $b$  is 2; for the higher energy transition its value is 1. Implementation of eq 4, using the absorption data in Figure 1 and Stark derived values for  $R_{ab}$ , yields coupling energies of  $1400$  and  $2560 \text{ cm}^{-1}$ , respectively, for optical ET from the osmium  $d_{xy}$  orbital and either the  $d_{xz}$  or  $d_{yz}$  orbital. The energy ordering is consistent with the orthogonal and parallel geometric assignments, above, but also points to the substantial degree of mixing that must exist in order for the nominally orthogonal transition to become so strongly allowed.<sup>17</sup> Both energies are substantially greater than the coupling energies that would be calculated if the charge transfer distance were naively identified with the metal–metal separation distance. The differences are

(14) (a) Reimers, J. R.; Hush, N. S. *J. Phys. Chem.* **1991**, *95*, 9773. (b) Shin, Y. K.; Brunschwig, B. S.; Creutz, C.; Sutin, N. *J. Am. Chem. Soc.* **1995**, *117*, 8668. (c) Shin, Y. K.; Brunschwig, B. S.; Creutz, C.; Sutin, N. *J. Phys. Chem.* **1996**, *100*, 8157.

(15) See: Brunschwig, B. S.; Ehrenson, S.; Sutin, N. *J. Phys. Chem.* **1986**, *90*, 3657. The mixed valence complex was treated as an ellipsoid with a semimajor axis  $12.4 \text{ \AA}$  in length, a pair of semiminor axes  $7 \text{ \AA}$  in length, and an interfacial distance of  $10.2 \text{ \AA}$ .

(16) An alternative approach with  $R_{ab}$  values of  $2.8$  and  $4.0 \text{ \AA}$  and fractional charge transfers of  $95\%$  and  $97\%$  leads to solvent reorganization energies of  $2200$  and  $4500 \text{ cm}^{-1}$ , respectively.

important, in part, because the coupling energy plays a key role in defining the reaction dynamics under nonadiabatic conditions, but also because the energy is significant in defining adiabatic reaction surface shapes (and therefore, reactivity) in the vicinity of diabatic surface crossings.<sup>18</sup>

### Conclusions

Electronic Stark effect measurements permit donor-orbital-specific one-electron transfer distances to be directly experi-

(17) We have assumed that the "perpendicular" transition gains linear absorption intensity exclusively via mixing of  $d(xz)$  and  $d(yz)$  donor (Os) orbitals with the  $d(xy)$  donor orbital. If other sources of intensity enhancement exist, then (a)  $H_{ab}(\text{perpendicular})$  almost certainly will be overestimated by eq 4, (b) the generalized Mulliken-Hush analysis will, strictly speaking, be inapplicable to the perpendicular component, and (c) the value above for  $R_{ab}(\text{perpendicular})$  will represent only an upper limit estimate (with  $R_{12}(\text{perpendicular})$  defining the lower limit). On the other hand, the conclusions regarding adiabatic charge transfer distance and solvent reorganization (derived from electroabsorption spectra) are not predicated upon specific assumptions concerning the mechanism(s) by which the perpendicular transition derives linear absorption intensity.

(18) For an erudite discussion see: Sutin, N. *Prog. Inorg. Chem.* **1983**, 30, 441.

mentally evaluated. The distances are remarkably dependent upon donor orbital orientation and significantly shorter than simple geometric estimates. From the distance information, donor-orbital-specific coupling energies and solvent reorganization energies can also be estimated. These likewise exhibit striking orientational dependencies, while differing substantially from parameters obtained by equating the charge transfer distance with the geometric donor/acceptor separation distance.

**Acknowledgment.** We thank the U.S. Department of Energy, Office of Energy Research, Division of Chemical Sciences (Grant No. DE-FG02-87ER13808), and the Dreyfus Foundation (Teacher-Scholar Award to J.T.H.) for support of this research. We also thank Chris Hutchinson for assistance with dielectric constant measurements, Dr. Vladimir Petrov for resonance Raman measurements, and Dr. Marshall Newton for helpful discussions.

JA963279L